F. W. Lichtenthaler and S. Immel

Computer simulation of chemical and biological properties of sucrose, the cyclodextrins and amylose

Reprinted from
International Sugar Journal, 1995, **97,**
(Issue No. 1153), 12 - 22.

INTERNATIONAL SUGAR JOURNAL

Computer simulation of chemical and biological properties of sucrose, the cyclodextrins and amylose[1]

By Frieder W. Lichtenthaler and Stefan Immel
(Institute of Organic Chemistry, Technical University of Darmstadt, Germany)

This article is based on the SPRI Science Award address presented on August 8th, 1994 at the Conference on Sugar Processing Research, Helsinki. Professor Lichtenthaler was given the award for his outstanding research and development work in sucrose science and technology.

He dedicates this account to Leslie Hough, one of the pioneers of sucrochemistry, on the occasion of his 70th birthday.

Summary.

Computer-aided models of the 3-dimensional molecular conformations are presented for sucrose, fructose, sucralose, non-carbohydrate sweeteners, cyclodextrins, and the amylose portion of starch.
The electropositive and electronegative areas on the contact surface of a molecule may be reliably determined and represented as a colour code, and similarly the hydrophilic and hydrophobic regions may be portrayed by computation of the molecular lipophilicity potentials (MLPs). Patterns of the MLP and the molecular electrostatic potential (MEP), visualised on the solvent-accessible surface in colour coded form, provide novel insights into the architecture of these molecules and their chemical properties (e.g. acidity of OH groups).

They also shed new light on how biological responses such as sweetness are triggered.

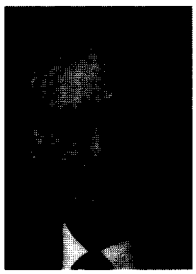

F. W. Lichtenthaler

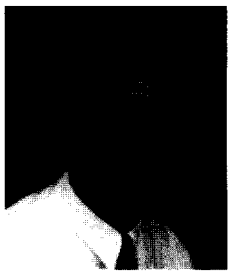

Stefan Immel

Introduction

Advanced computer modelling techniques may be applied to the elucidation of the individual conformations of carbohydrates in vacuum and in solution[2]. The possibility of representing various properties on the contact surface of sugars[3-4] has added a new dimension to their visual perception. Accordingly, not only may the electropositive and electronegative areas on the surface of a sugar molecule be reliably determined by computational methods, but the hydrophilic and hydrophobic regions as well[3,4].

Such information is particularly useful for understanding, and hence predicting, hydroxyl group reactivities in sugars. They are similar or nearly identical in the majority of cases. An insight into the relative acidities of the individual hydroxyl groups may be gained from the pattern of the molecular electrostatic potential (MEP) on the contact surface of a sugar. This is appropriate for planning selective entry reactions into useful derivatives.

In a similar fashion, reliable knowledge on where a mono- or disaccharide is hydrophobic is in principle obtainable from computation of its MLP's (molecular lipophilicity potentials). This has major implications on its biological properties, inasmuch as the "docking" of a substrate in a receptor (e.g. sucrose in the taste bud) is governed by hydrophobic interactions between the respective part of the substrate and the complementary hydrophobic section of the receptor protein. The biological response (i.e. sweetness in the case of sucrose) is elicited only when this docking is complete, most probably by hydrogen bonding via another part of the substrate.

To secure the MEP's and MLP's of simple sugars and disaccharides is thus a most helpful tool with which to plan chemical reactions of high potential selectivity. Understanding their biological processes on a molecular level has the ultimate aim of modifying their biological response (e.g. intensifying sweetness).

This account gives an overview of the present state of computer-aided modelling to visualize the conformations, the solvent accessible surfaces and the MEP's and MLP's of simple sugars such as sucrose. Non-carbohydrate sweeteners are included for comparison and these investigations are extended to the cyclodextrins and the amylose portion of starch in order to get a better understanding of their molecular architecture and their properties.

Conformation of sucrose in the solid state and in solution

The common sucrose formula (Fig. 1, left) does not give any three-dimensional information about the actually predominating conformation[3]. A more 'realistic' molecular picture is obtained from neutron diffraction[5], and from X-ray analysis[6] of the solid-state conformation (Fig. 1, right), showing the glucose and fructose moiety fixed in their relative orientation by two strong interresidue hydrogen bonds between 5-O^g ... HO-6^f and 2-O^g ... HO-1^f of 1.89 and 1.85 Å length, respectively.

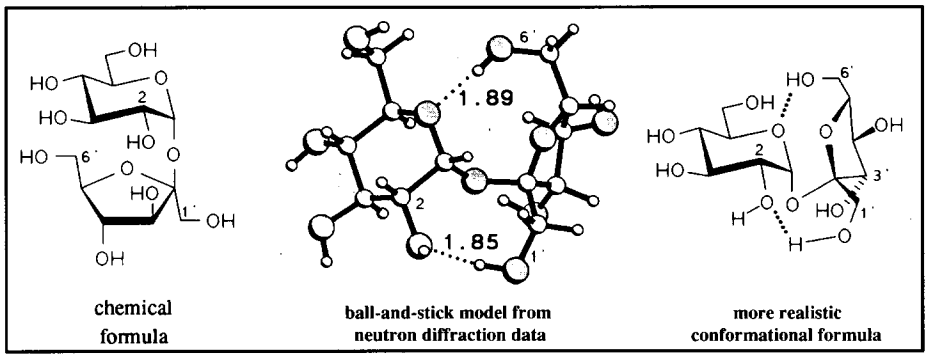

Fig. 1. Representations of the solid state conformation of sucrose

In solution, particularly in water, it is unlikely that both intramolecular hydrogen bonds of the crystalline state are retained. Extensive ^{1}H- and ^{13}C-NMR investigations[7-11] strongly attest to the disintegration of the 5-O^{g} ...HO-6^{f} hydrogen bond by solvation, despite the fact that a more recent NMR study concludes that there is no intramolecular hydrogen bond in sucrose in aqueous solution[12]. Detailed optical rotation data of aqueous sucrose solutions[13], however, are best accounted for in terms of an equilibrium mixture of two conformers. The predominant one is similar to the crystalline structure in which the 2-O^{g} ... HO-1^{f} hydrogen bond persists (Fig. 2, left), and the other features a 2-O^{g} ... HO-3^{f} bond (Fig. 2, right).

This contention is in accord with conclusions, reached on the basis of steady state NOE's and long-range ^{13}C-^{1}H couplings, that sucrose in aqueous solution maintains the 2-O^{g} ... HO-1^{f} intersaccharidic hydrogen bond[7], as well as with NMR-based reasonings that, in DMSO solution, a 2:1 equilibrium of the two conformers prevails[10].

A variety of computational methods and force fields have been used for the theoretical treatment of sucrose to unravel its minimum energy conformations, such as HSEA[7], PFOS[14], CHARMM[15,16], PIMM88[17] and MM3[18]. Despite the fact that the locations and relative energies of the minima differ to some extent, some trends are independently reproduced by all studies. The intersaccharidic torsion angle Φ, representing rotation around the axially oriented anomeric C_{1g}-O_{1} bond of glucose, is considerably more restricted than Ψ, which describes the flexibility around the alternate pseudoequatorial C_{2f}-O_{1} anomeric bond of the fructose portion (Fig. 3).

In all cases, three main families A - C of sucrose minimum energy conformers are found, with Φ almost invariably in the range of +80° to +100°, whilst Ψ ranges from -40° to -90° (class A), +170° to -170° (B) and +50° to +70° (C). Thereby, the global minimum energy conformer (class A) resembles closely the solid state conformation, and the minima B and C are higher in energy by 8 - 25 kJ/mol.

These rationalizations, from the bulk of calculatory evidence accumulated to date, correspond to our results obtained with the PIMM88 force field program[19], which appears to be particularly well suited for the treatment of overlapping anomeric effects.

Computation of the fully relaxed energy potential surface provided three local energy minima for sucrose in a percentage distribution of 71: 21: 8%[17]. The molecular geometries of these conformers are depicted in Fig. 4 and the two major ones are given in Fig. 5 in ball and stick representation, with their contact surfaces shown in dotted form. The major conformer (Fig. 5, left) is characterized by its 2-O^{g} ...HO-1^{f} bond, the minor one (right) features the 2-O^{g}...HO-3^{f} alternative, whilst the geometry of the third (8% of the population only) is determined by a hydrogen bond between the fructose 3-OH and the glucose ring oxygen .

It is to be noted that these two principal conformers emerging from our PIMM calculations correspond closely to those delineated by the NMR and rotational data mentioned above (Fig. 2). Accordingly, we have based our modelling of the electrostatic and hydrophobic properties on these two molecular geometries.

Contact surface and molecular electrostatic potential (MEP) profile of sucrose

The molecular geometries elaborated above for sucrose should be tested, i.e. whether they are able to explain or even predict chemical and biological properties. With this in mind, we have generated, by use of the MOLCAD program[20], the so-called contact surfaces of these conformers (dotted areas in Fig. 5) relative to water molecules, i.e. 'how water sees sucrose'. For each of these dots on the surface, the Molecular Electrostatic Potential (MEP) was calculated (i.e. how positive or negative in electrostatic terms such a surface point is). The respective numeric values were transferred into a color-code for visualization[17].

The resulting MEP patterns for each of the two relevant sucrose conformers are given in Fig. 6. As is clearly evident, the area of the 2-OH group of the glucose portion (the most intense red part of the surface) is the one with the

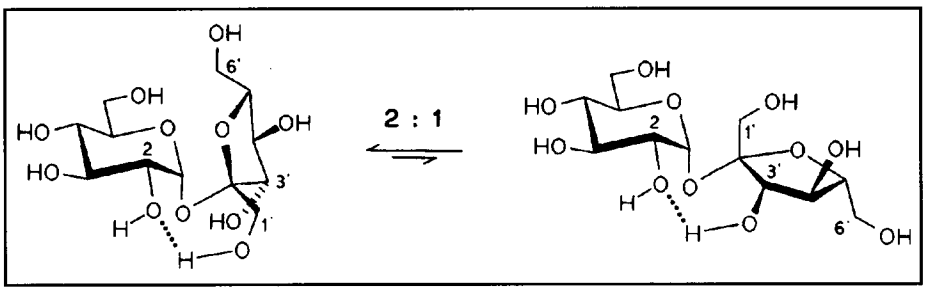

Fig. 2. Conformations of sucrose in DMSO solution, showing a competitive equilibrium between two forms

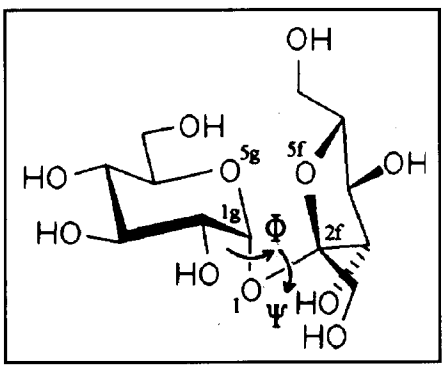

Fig. 3. Sucrose: definition of intersaccharidic torsion angles Φ and Ψ

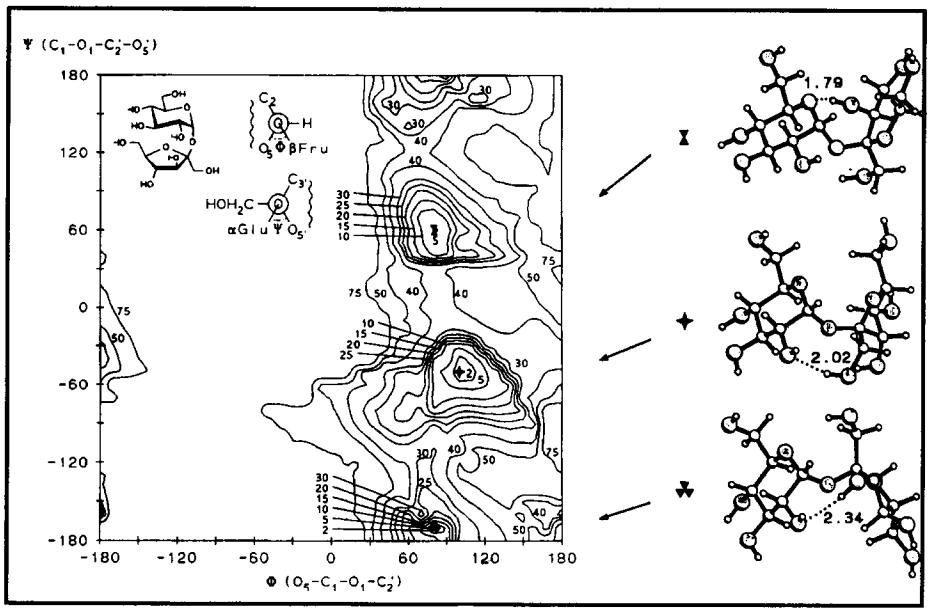

Fig. 4. Fully relaxed energy potential surface of sucrose as a function of the two intersaccharidic torsion angles Φ and Ψ, in kJ/mol relative to the global minimum. The energy minimum at Φ ≈ +110°, Ψ ≈ -50° corresponds closely to the solid state conformation

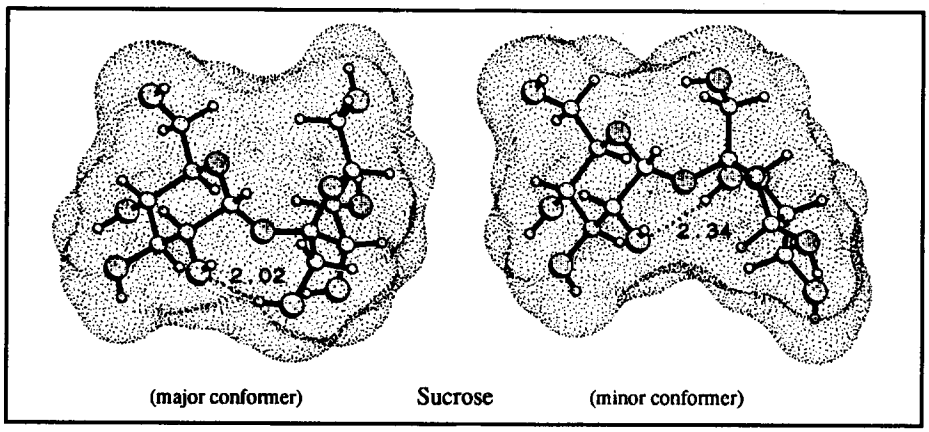

Fig. 5. Ball and stick model of the low energy conformers of sucrose showing the contact surface in dotted form. They are likely to represent the conformations prevailing in solution (cf. Fig. 2)

highest positive electrostatic potential. The strong positivation of the glucosyl-2-OH must lead to enhanced acidity of this hydroxyl group over the others, i.e. on treatment with a base, it should be deprotonated first. There is ample experimental evidence for this. It has been demonstrated[21] that 2-O-acyl and 2-O-(N-carbamoyl)-derivatives of sucrose are obtained in useful yields by NaH-deprotonation of sucrose in pyridine and reactions with 3-acylthiazolidinethiones. Our studies[22] on this NaH-induced deprotonation of sucrose and subsequent exposure of the mono-anion to benzyl bromide in DMF opened up a route to 2-O-benzyl-sucrose, adaptable to a large scale. On reaction with benzyl bromide a 9: 2:1 mixture of monobenzyl ethers is generated, which are the 2-O-benzylated product (major), and the fructose- l'-O- and 3'-O-benzyl isomers (minor). Similar regioselectivities are observed on electroreductive deprotonation of sucrose within the cathodic compartment of an electrolysis cell and the subsequent trapping of the mono-anion by alkylation or acylation[23]. All these findings agree with the MEP-derived predictions and, in turn, provide evidence for the retention of intramolecular hydrogen bonding in sucrose in solution (at least in DMF solution). The interresidue 2-O^g ... HO-1^f and 2-O^g ... HO-3^f hydrogen bonds in sucrose not only determine the MEP profiles, i.e. the electropositive 2-OH proton, but are also responsible for the stabilization of the anion at these positions[17].

Molecular lipophilicity potential (MLP) profiles of sucrose

The interactions of sugars with receptor proteins are not only governed by electrostatic effects, including hydrogen bonding, but also by dispersion forces (van der Waals contacts) and hydrophobic effects. However, when looking at standard space-filling models, assessment of these interactions, i.e. the areas that might be hydrophobic, is difficult. Utilizing the MOLCAD program[20], the molecular lipophilicity potentials (MLP's) can be calculated on molecular surfaces, i.e. the hydrophobicity portraits of the molecules.

Applying this methodology to sucrose[3,24], the MLP profiles for both conformers were generated and the computed values were transferred into 32 colour shades (Fig. 7). 16 colours ranging from dark blue (most hydrophilic) over light blue to full yellow (most hydrophobic) were used for mapping the computed values on the surface. The remaining 16 colour shades (light blue to brown) were used to indicate iso-contour lines in between the former colour scale, allowing a more quantitative assessment of relative hydrophobicity.

For the major sucrose conformation in Fig. 7 (far left), the hydrophilic and hydrophobic portions of the molecule are distinctly separated on opposite sides. The half-opened form with the stick and ball model inserted clearly reveals the entire outside section of the fructose moiety to be hydrophobic (i.e. yellow),

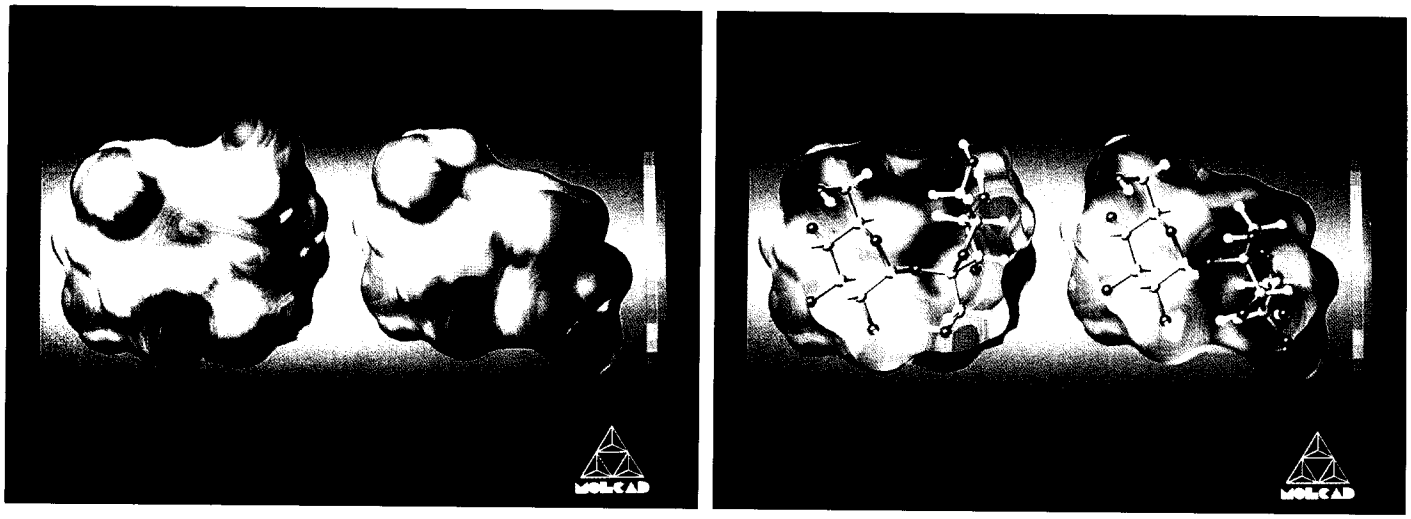

Fig. 6. Colour-coded representation of the molecular electrostatic potential (MEP) profiles of the two relevant sucrose conformers (see Fig. 5). The 16-colour code ranges from violet (most negative potential) to red (most electropositive). The opened forms on the right show a ball-and-stick model inserted

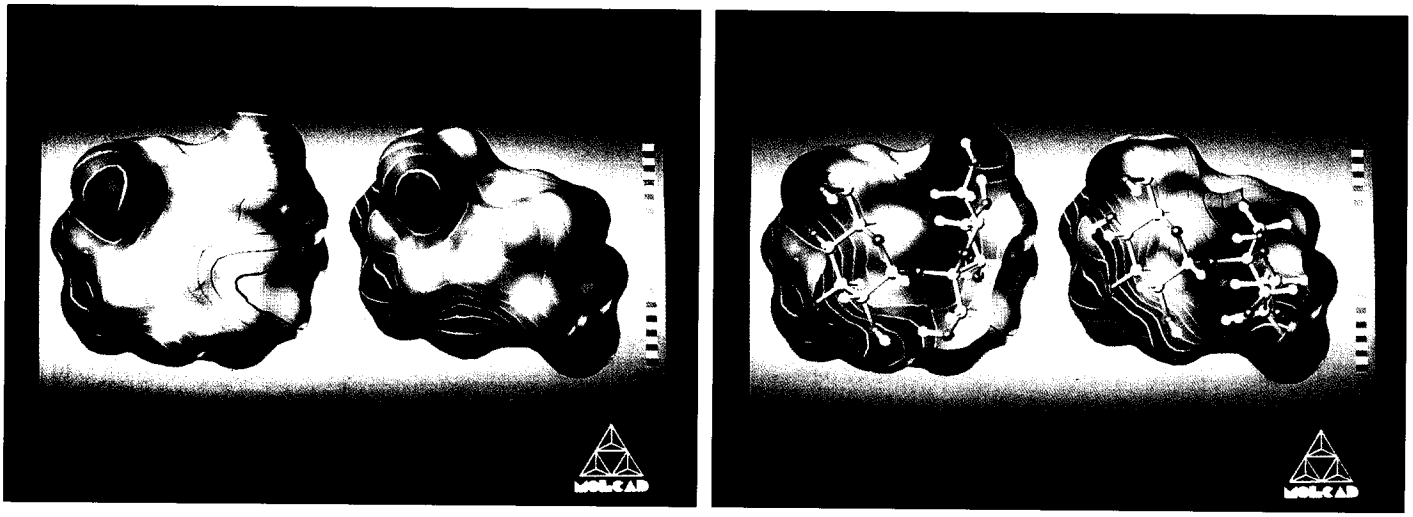

Fig. 7. Molecular lipophilicity profiles for the two sucrose conformers of Fig. 4, blue corresponding to hydrophilic surface areas and yellow to the most hydrophobic regions. For both conformers the entire 'back side' of the fructose moiety is decisively hydrophobic

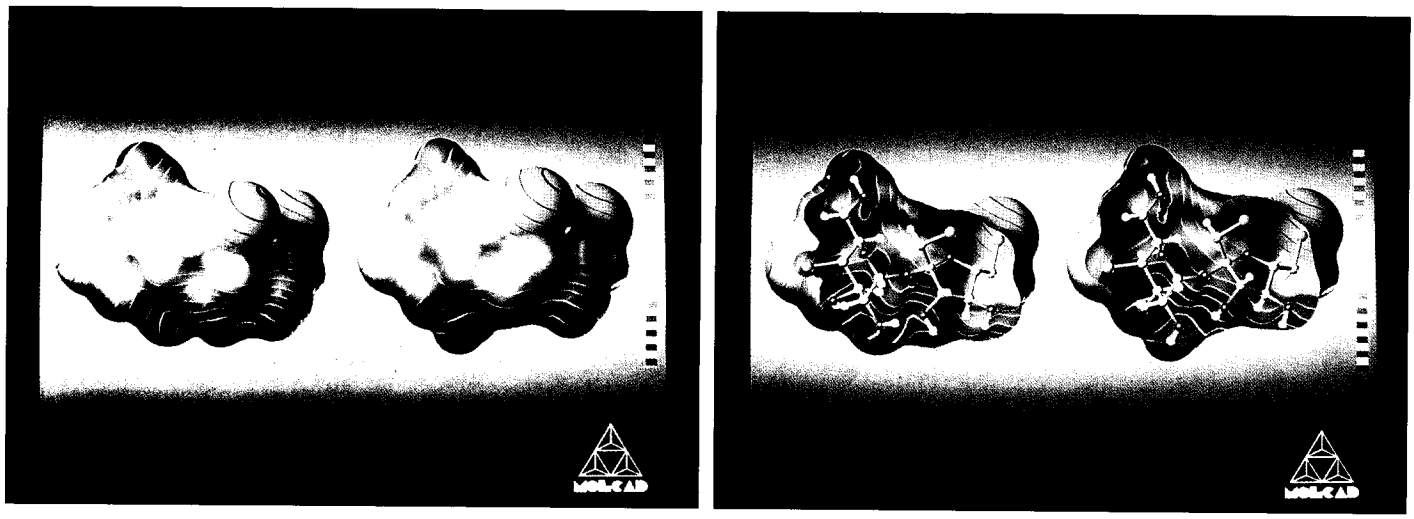

Fig. 11. Molecular lipophilicity potential (MLP) of sucralose in the solid state. The X-ray structure[56] derived form is far left and the computer-simulated form is next to it. The reversal of the direction of the bond from 2-OH^{g}...O-3^{f} (left) to 2-O^{g}...HO-3^{f} (right) results in a concentration of the hydrophilic area (blue) around O-2^{g}

and the blue hydrophilic section to be centred around the 3-oxygen of glucose.

The other likely to prevail sucrose conformation in solution is similar except that the hydrophobic region located at the outer side of the fructose moiety is now more compact. Consequently, that part of sucrose able to engage in hydrophobic binding within the sweet-taste receptor is an entire region of the fructose portion, rather than a specific position .

Biological significance of MLP profiles of sucrose

Sucrose being actively transported in plants, its recognition binding to the carrier proteins is governed not only by complementary geometries of substrate and receptor, but by similar or even identical topographies in hydrophilic/ hydrophobic terms. The same applies to the elicitation of the sweetness response by sucrose in the taste bud. Knowing the relevant hydrophilic and hydrophobic regions on the contact surface, from the MLP patterns, sheds new light on how the sweetness sensation is triggered on a molecular level.

The classical attempt by Shallenberger[25] and Kier[26] to rationalise the sweet taste of organic compounds presumes the existence of a common AH-B-X glucophore in all sweet substances [comprising a hydrogen bond donor (AH) and acceptor functionality (B), as well as a hydrophobic binding point (X), Fig. 8]. This elicits the sweetness response via the inter-action with a complementary tripartite AH-B-X site in the taste bud receptor[27].

However, this theory, also termed the 'sweetness triangle', appears much too simple to explain all the observations, particularly bearing in mind that sweet-taste perception is mediated by a cascade of complex biochemical processes[28-31] that are little understood at the cellular level. Nevertheless, the tripartite AH-B-X glucophore concept has proved useful (despite not being three-dimensional) in rationalizing structure-sweetness relationships in such diverse compounds as amino acids, dipeptides, sulfamides (e.g. saccharin and acesulfame), and sugars including sucrose and fructose.

In the case of sucrose, for example, there have been uncertainties in placing the sweetness triangle, i.e. in correlating the respective AH-, B-, and X-parts to distinct parts of the molecule. Assignments A3233 (Fig. 9, left) and B34 (Fig. 9, right) - from the original literature - have been proposed, but neither has been able to explain the sweetness characteristics of a large number of sucrose derivatives, nor do they have any predictive value[27].

The MLP patterns in Fig. 7 provide ample evidence that there is not a single hydrophobic binding point, as implied by the sweetness triangle concept, but an extended hydrophobic region in the sucrose molecule, encompassing the entire back side of the fructose portion. Moreover, the hydrogen bonding AH-B-couple must be contained in the opposite hydrophilic region of the molecule. The location of the tripartite AH-B-X glucophore therefore emerges in the form shown in Fig. 10[24].

Accordingly, the AH-B-couple is represented by the glucosyl-2- and 3-OH groups, of which the distinctly electropositive glucosyl-2-OH (cf. Fig. 6) is energetically most favoured to engage in hydrogen bonding as a donor, and may be assigned as the AH-unit. The hydrogen bond acceptor (B-unit) must be located nearby, pointing to the

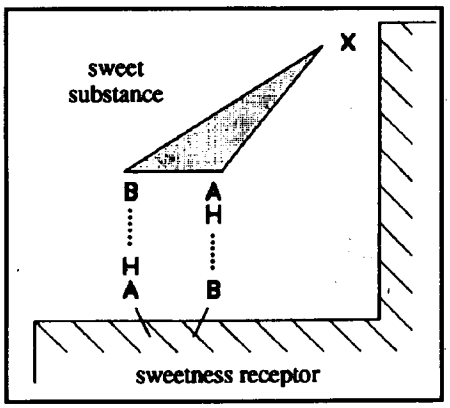

Fig. 8. Shallenberger/Kier concept of structure-sweetness relationships ('sweetness triangle')

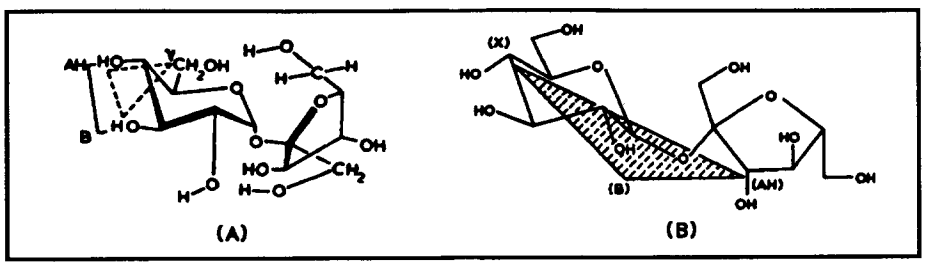

Fig. 9. AH-B-X-glucophore assignments for sucrose as proposed by Mathlouthi *et al.*[32,33] and by Hough *et al.*[34]

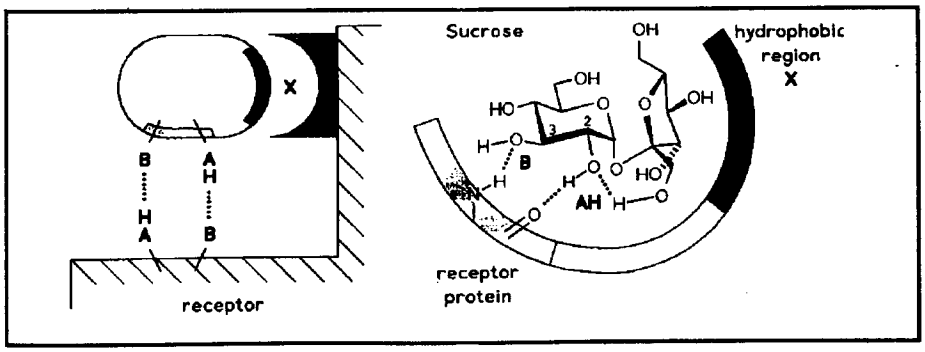

Fig. 10. Modified AH-B-X-concept of sweetness (left) with an extended hydrophobic region X rather than a specific binding point, and the opposite side-located hydrophilic AH-B-couple. In sucrose (right), the AH-B-couple is represented by the glucosyl-2- and 3-OH groups, while the entire back side of the fructose contributes to the hydrophobic interaction with the sweetness receptor

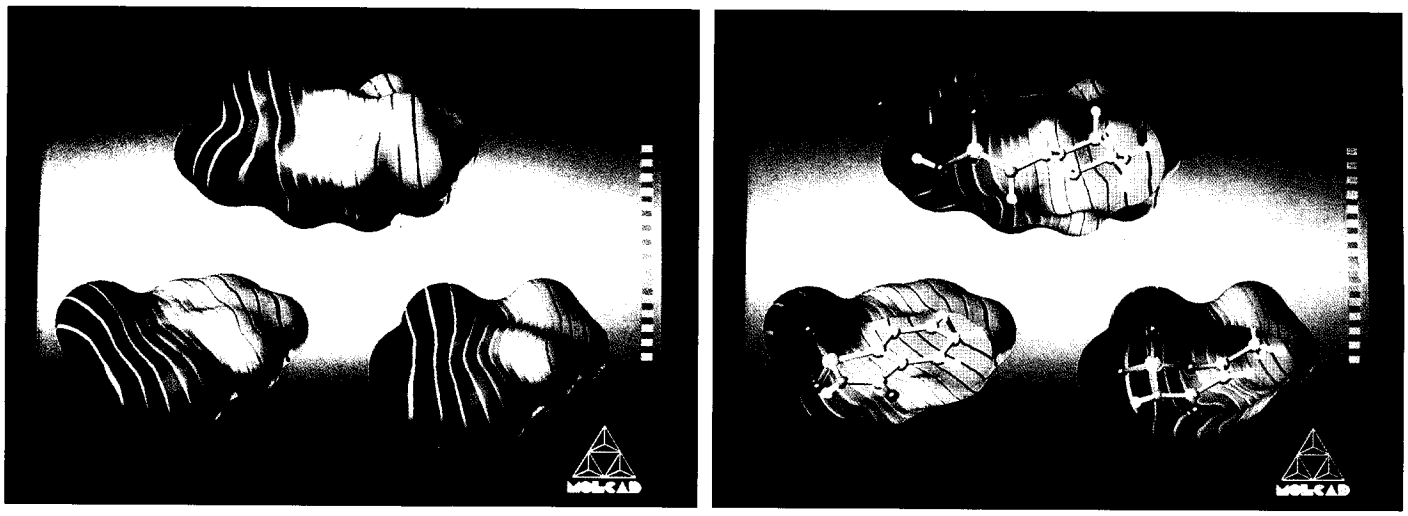

Fig. 12. MLP profiles (yellow: hydrophobic, blue: hydrophilic) for the sulfamide sweeteners cyclamate (A, upper), saccharin (B, lower left), and acesulfame (C, lower right) in closed and opened form. A was generated by force field calculations, and B and C were modelled according to the X-ray structural data of the corresponding sodium or potassium salts[36-38]

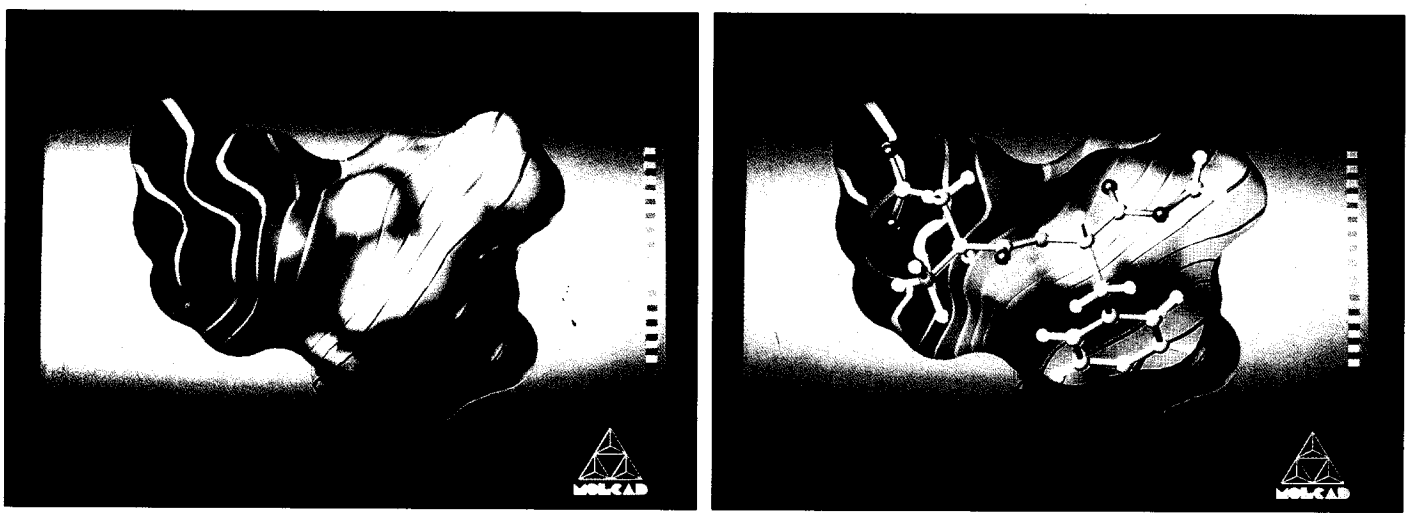

Fig. 13. The MLP profile of the dipetide sweetener aspartame in the solid state conformation[39], showing the hydrophobic region to be determined by the benzene ring of the phenylalanine part and the hydrophilic area is again on the opposite side

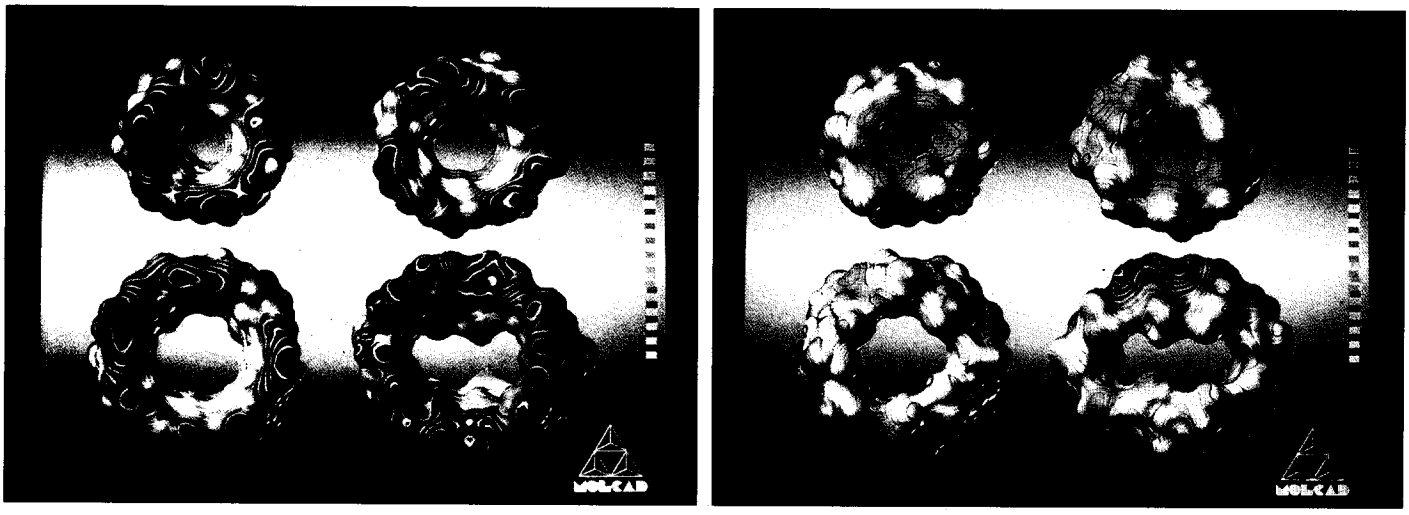

Fig. 15. MLP profiles of α-CD (upper left), β-CD (upper right), γ-CD (lower left), and δ-CD (lower right)[42-45] in their solid state conformations. The left picture views through the larger openings of the conically-shaped molecules, while the right depicts the 'back' side

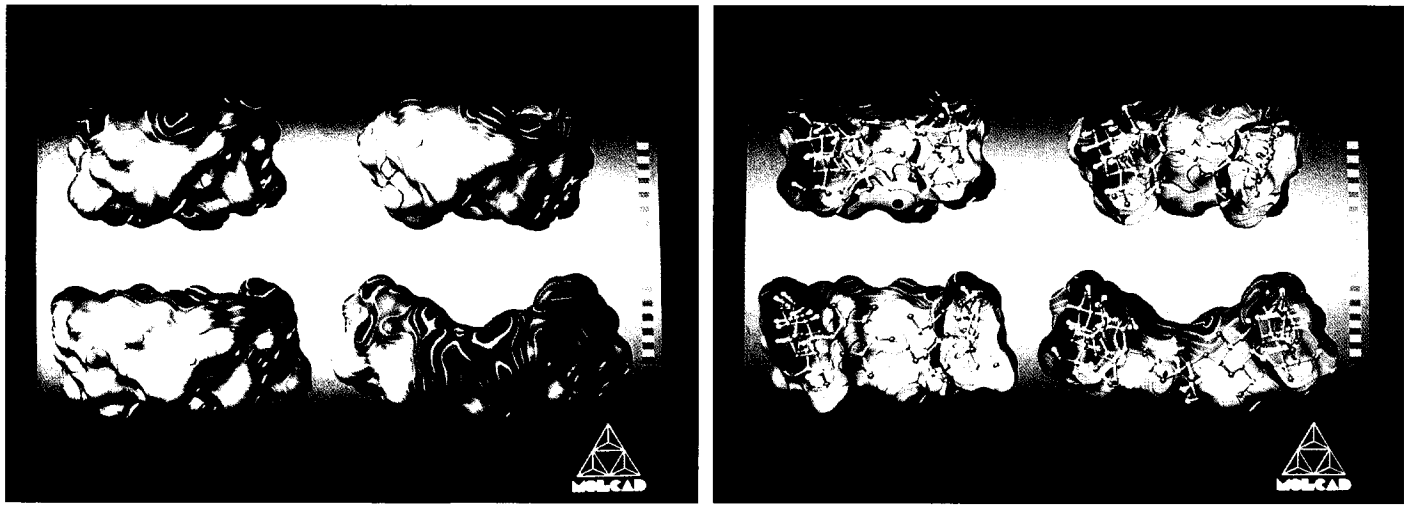

Fig. 16. Side view MLP's, each in closed and bisected form , of the four α(1→4)-cyclodextrins. The 2-OH/3-OH side is aligned upward (larger opening of the torus) and the CH_2OH groups point downward (smaller aperture). The similar hydrophilic and hydrophobic areas are apparent, and the elliptically distorted U-shape of δ-CD

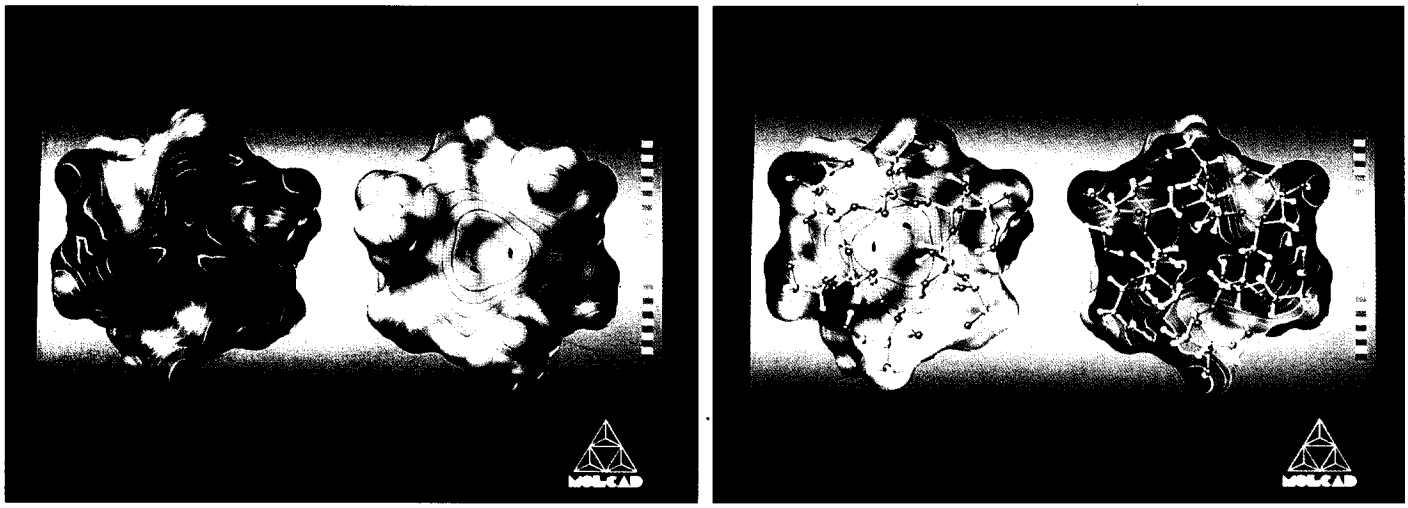

Fig. 18. MLP profile (blue: hydrophilic, yellow: hydrophobic) of α-cyclofructin; the half-opened models with a ball-and-stick model inserted illustrate the molecular orientation. In the left models, the 3-OH^f and 4-OH^f fructofuranose residues point towards the viewer, and the right models are rotated by 180°

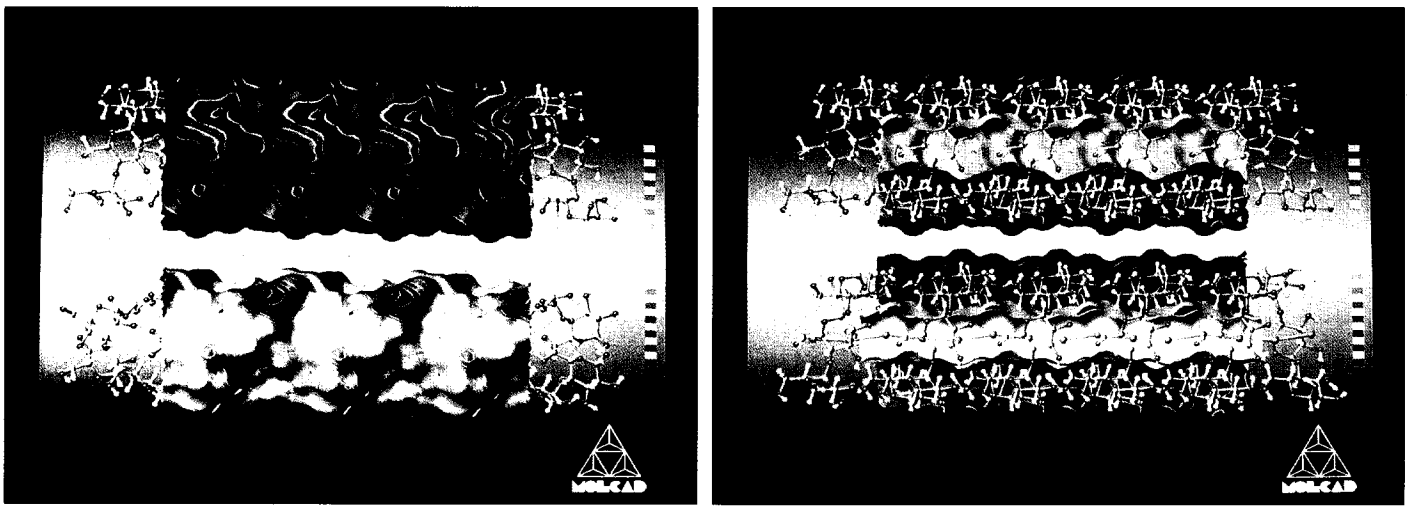

Fig. 19. Hydrophobic topographies for the amylose fraction of starch, showing fragments of approximately 30Å length, with the surfaces for the centre sections of the rod-shaped polymers only. The single stranded V_H-amylose (upper) is set against the parallel-stranded double-helical A-form (below). The half-opened model of V_H-amylose reveals the hydrophobic centre channel

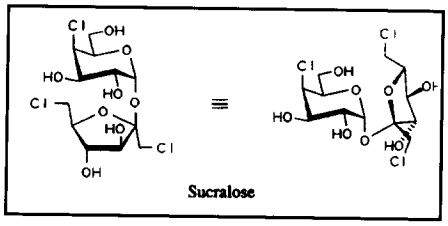

glucosyl-3-OH as the most likely candidate. The X part is represented by the entire back side of the fructose residue that contributes to the hydrophobic interaction with the sweetness receptor.

MLP profiles of sucralose and some non-carbohydrate sweeteners

Whilst absolute proof for the modified AH-B-X assignment to sucrose is necessarily lacking as long as the topography of the receptor is not known in detail, it is supported by the sweetness characteristics of altogether 53 sucrose derivatives. They correlate well with this concept in terms of structure-sweetness relationships[24], not only in geometrical terms but also in the hydrophilic/ hydrophobic profile. Most notably, the intensely sweet sucralose (650× sucrose) a trichloro-derivative of galacto-sucrose, shows an MLP profile (Fig. 11), in which the two chlorine atoms of the fructose portion turn out - expectedly - to be the most hydrophobic (yellow) regions (X-area).

Another obvious similarity with sucrose is the fact that hydrophobic (yellow) and hydrophilic (blue) regions are located on opposite sides of the molecule, seemingly little disturbed by the third chlorine in the galactose portion, which Fig. 11 shows is substantially less hydrophobic than the other two halogen atoms.

To further test our modified AH-B-X concept, it was obvious to extend the MLP pattern approach to other sugars, e.g. fructose (with favourable results[35]) and to non-carbohydrate high-potency sweeteners, such as cyclamate, saccharin, acesulfame, and aspartame.

In the case of the three sulfamides, the similarity of their respective hydrophobicity (MLP) patterns is amazing (Fig. 12). That the sulfamido grouping is the hydrophilic portion of the molecule is to be expected. That a cyclohexyl ring (in cyclamate), an aromatic moiety (as in saccharin) and an acetoacetyl residue fixed in the enol form (as in acesulfame) yield hydrophobic areas closely resembling each other is most remarkable. The two lower representations in Fig. 12, corresponding to saccharin and acesulfame, are essentially identical.

Another striking feature is that hydrophobic and hydrophilic portions of the molecules are on opposite sides, as in the case of sucrose and sucralose . Moreover, the very same distinct separation of hydrophilic and hydrophobic areas is observed for the dipeptide sweetener aspartame (Fig. 13). The most hydrophobic region originates from the aromatic ring of the phenylalanine part, whilst the amino-carboxylic acid part at the opposite side of the molecule is seemingly responsible for the hydrophilic area. The protrusion made up by the methoxycarbonyl ($COOCH_3$) group, not involved in binding, is apparently readily adapted by the sweetness receptor.

All of this sustains the notion that the receptor - be it the same for sucrose, fructose, and non-carbohydrate sweeteners or different - is quite flexible in adapting to the hydrophobic portion of sweet substances, i.e. to the X part, which is clearly not a specific position of the molecule, but an entire region. If this hydrophobic area is the main factor governing the 'docking procedure' of the sweet substance, i.e. directing it to and locking it into the complementary 'hydrophobic cleft' of the receptor protein, it can well be imagined that the hydrophilic area on the opposite site, (likely to contain the AH-B portion of the Shallenberger-Kier glucophore), is positioned to elicit the sweetness response via hydrogen bonding to a complementary receptor site AH-B couple.

In summary, much remains to be learned about the intricacies of the mechanisms involved in activation of sweet-sensitive cells, and direct evidence is urgently required. Nevertheless, the consideration of the three-dimensional shape of sweet molecules, their contact surfaces and particularly their MEP and MLP profiles, has provided a new dynamic vision, not only of the sweet molecule as such, but also of its complementary binding site. This may lead, via computer-aided receptor modelling, to more realistic structure-sweetness concepts.

Hydrophobicity potential profiles of cyclodextrins

The starch-derived cyclodextrins (CD's) are a group of cyclic oligosaccharides containing six, seven, eight or nine α(1→4)-linked D-glucopyranose units per molecule. They have unusual bucket-shaped loop structures, a feature that allows them to

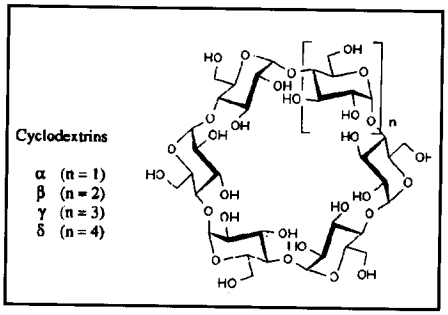

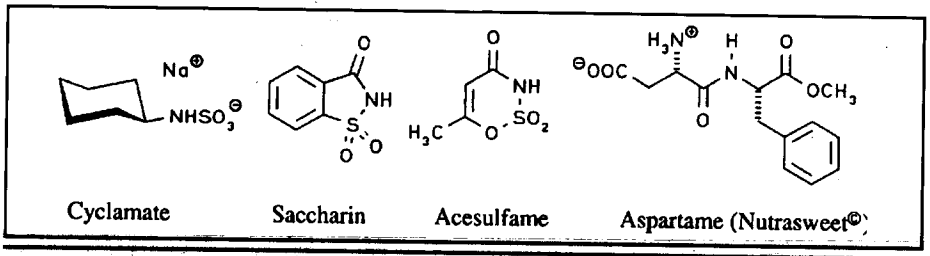

form inclusion complexes by insertion of a wide variety of organic molecules into their hydrophobic intramolecular cavity[40-41].

Their molecular geometries were generated, starting from the respective X-ray structures of the hydrates[42-45], which were allowed to 'float' with the PIMM-program to obtain the minimum energy conformation depicted in Fig. 14. Onto this the contact surfaces were superimposed in dotted form[1,46,47], as for sucrose.

The successive enlargement of the central cavity when increasing the number of glucose units from six in the cyclic hexasaccharide (α-cyclodextrin, top left) to seven (top right), eight and nine (below) is as obvious as the fact that the largest one features a spectacle-shaped cavity rather than circular[47].

That these cyclodextrin cavities exhibit hydrophobic properties is well established on the basis of their ability to form 1:1 inclusion complexes, yet a clear indication which areas are hydrophobic or hydrophilic - the cyclodextrins are fairly soluble in water - can not be derived from chemical formulae, models or contact surfaces. Generation of their hydrophobicity potential profiles in the same way as for sucrose provides a most impressive, lucid picture of how these cyclodextrins are balanced with respect to their hydrophilic (blue) and hydrophobic (yellow) areas (Fig. 15). One side of these molecules, i.e. the larger opening of the bucket-shaped macrocycle, carrying the secondary glucose 2-OH and 3-OH groups, is intensively hydrophilic (Fig. 15, left), whilst the alternate narrower side (right, containing all of the primary CH_2OH groups) is considerably less hydrophilic, partially permeated by yellow (hydrophobic) areas. An even clearer impression of the MLP patterns is provided by the side-views in closed and half-opened form (Fig. 16). The bulk of the hydrophobic regions, however, is concentrated in the inner of the cavities, which is particularly obvious in the highly symmetric γ-cyclodextrin (lower left).

Accordingly, the complexation of the cyclodextrins with suitable guest molecules, which is governed by a variety of factors - steric fit, van der Waals, electrostatic and hydrophobic interactions - can be rationalized with respect to the latter ones on the basis of their MLP profiles. A detailed elaboration is forthcoming[47].

Cycloinulin: geometry and hydrophilic topography

Enzymatic degradation of inulin, a β(1→2)-linked polymer of D-fructofuranose from Dahlia and Jerusalem artichoke tubers, provides - analogous to the generation of the cyclodextrins from starch - cyclooligosaccharides consisting of six, seven or eight fructose residues[48,49], which are, accordingly, designated as β(1→2)-linked cyclofructins. The most readily accessible of these cyclofructins is the hexamer (Fig. 17).

Based on its X-ray structure[50], the molecular geometry of the macrocycle is depicted on the right. The contact surface, generated via the MOLCAD methodology, reveals a topography devoid of an interior cavity[46]. The color-coded MLP profile (Fig. 18,) indicates a distinct hydrophilic/hydrophobic differentiation between front and back side of the macrocycle. Due to the

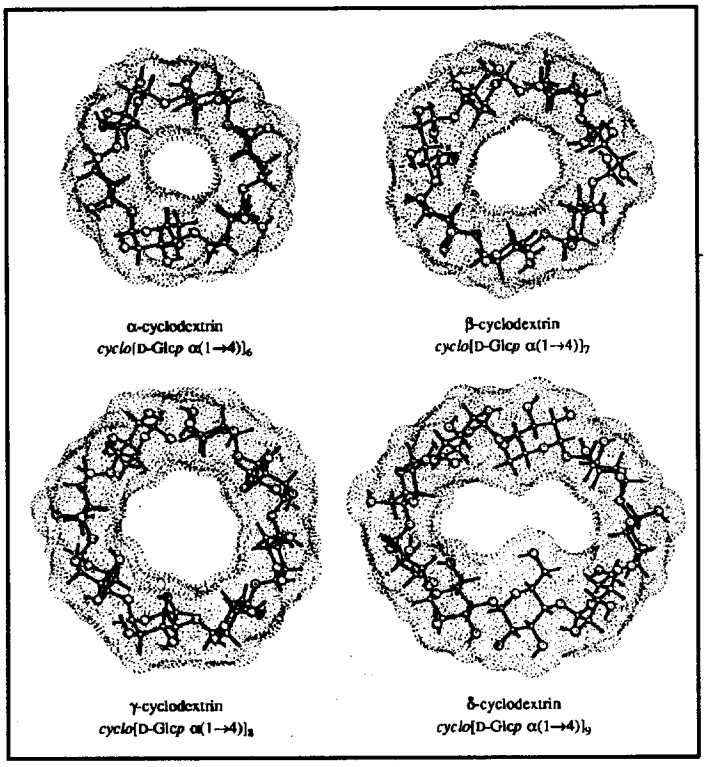

Fig. 14. Solid state molecular geometries and dotted contact surface of α- (upper left)[42] β- (upper right)[43], γ- (lower left)[44], and δ-cyclodextrin (lower right)[45]

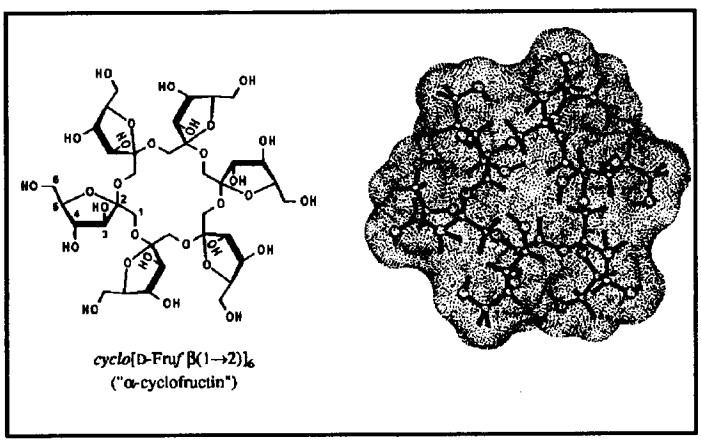

Fig. 17. Chemical formula of α-cyclofructin (left) consisting of six β(1→2)-linked fructofuranose residues, and representation of its solid state structure[50] (right)

location of the fructosyl-3- and 4-OH groups as well as the O-l^f of the intersaccharidic linkage on the same ('front') side of the molecule this surface region is distinctly hydrophilic (Fig. 18, far left). The opposite side is determined by the l-CH_2, 6-CH_2 and 5-CH fragments, and, accordingly, entails a distinctly hydrophobic back side, with an indentation in the centre[46].

In consequence, the hexameric β(1→2)-cyclofructin is not capable of forming inclusion complexes with guest molecules, yet its decisively hydrophobic indentation on one side of the macrocycle is open for potential binding with complementary guests. Conceivably, the cyclofructin composed of eight β(1→2)-linked fructofuranose residues exhibits a hydrophobic cavity large enough to allow penetration of hydrophobic guest molecules.

The hydrophobic topography of amylose

Different structural models have been put forth for the amylose portion of starch. For V_H-type amylose, single-stranded left-handed helices with 6 glucose units per turn have been proposed on the basis of X-ray diffraction studies[51], while the A-form seems to consist of left-handed parallel-stranded double helices[52]. Both geometries and the pathway of transition between them are still subject to discussion[53].

Using the same MOLCAD program methodology as employed for sucrose and the cyclooligosaccharides, the helical V_H-amylose and double-helical A-form structures were generated, with their respective MLP profiles.

As is clearly apparent from the color-coded representations in Fig. 19, the hydrophobic characteristics of the V_H-amylose (top) and the A-form (bottom) differ significantly, the latter exhibiting an irregular distribution of hydrophobic and hydrophilic surface areas due to the absence of an inner channel. This is distinctly contrasted by the outside surface regions of the V_H-amylose, which are highly hydrophilic (blue) while its center channel is decisively hydrophobic (yellow) shown in opened form on the right. The hydrophobic characteristics are in accord with the experimental finding that amylose can form inclusion complexes with fatty acids by incorporation of their alkyl chains into the hydrophobic channel[54]. Also the formation of the dark blue-stained amylose iodine complex is caused by inclusion and an essentially perfect linear alignment of iodine/iodide in the hydrophobic centre channel according to the solid state structure obtained from X-ray diffraction[55].

Acknowledgements

We are grateful to Prof. Dr. J. Brickmann of the Institute of Physical Chemistry of the University of Darmstadt, for kindly granting us access to his MOLCAD program and the Silicon Graphics workstation.

Simulación por computador de las propiedades químicas y biológicas de sacarosa, ciclodextrinas y amilosa

Se presenta un modelo asistido por computador de los perfiles de conformación, potencial electrostático molecular (MEP) y potencial lipofílico molecular (MLP) para sacarosa, fructosa, endulzantes no carbohidratados, ciclodextrinas y la porción de amilosa del almidón. La representación de sus patrones MEP y MLP sobre la superficie del solvente en forma de colores codificados proporciona nuevos conocimientos de la arquitectura molecular de estos compuestos, sus propiedades químicas (por ejemplo, acidez de grupos OH) y las interacciones con el receptor para dar respuestas biológicas tales como la dulzura.

Simulation par ordinateur des propriétés chimiques et biologiques du saccharose, cyclodextrins et amylose

On présente un modèle assisté par ordinateur des profils des conformations, le potentiel électrostatique moléculaire (MEP) et le potentiel lipophilique moléculaire (MLP) pour saccharose, fructose, édulcorants non-hydrates de carbone, cyclodextrins et la portion d'amylose de l'amidon. La représentation de leurs modèles MEP et MLP sur la surface du solvant sous forme de couleurs codifiées offre une compréhension nouvelle de l'architecture moléculaire de ces molécules, leurs propriétés chimiques (par exemple l'acidité des groupes OH), et les interactions avec le récepteur pour donner les réactions biologiques telles que le goût sucré.

Computersimulierung der chemischen und biologischen Eigenschaften von Saccharose, der Cyclodextrine und Amylose

Dargestellt werden die computergestützte Modellierung der Konformationen und die Profile des molekularelectrostatischen Potentials (MEP) und des Molekularlipophilizitätspotentials (MLP) von Saccharose, Fructose, nicht Karbohydrat-Süßstoffe, Cyclodextrine und des Amyloseanteils von Stärke. Die Sichtbarmachung ihrer MEP- und MLP-Bilder auf der für Lösungsmittel zugänglichen Oberfläche in farbcodierter Farm bietet einen neuartigen Einblick in die Architektur dieser Moleküle, die Rezeptorwechselwierkungen bei der Entlockung von biologischen Reaktion wie z.B. bei der Süßigkeit.

1 This paper is considered to be Part 5 of the series *"Molecular Modelling of Saccharides"*. Part 4: F.W. Lichtenthaler and S. Immel: *Tetrahedron Asymmetry*, 1994, 5, in press.

2 French & Brady (Eds.): *"Computer Modelling of Carbohydrate Molecules"*, ACS Symposium Series 430, Am. Chem. Soc.,

Washington, D.C., **1990.**
3 Lichtenthaler *et al.: Starch/Starke,* 1991, **43,** 121 - 132; *Shokuhin Kogyo* 1992 *(The Food Ind. Jpn)* 1991, **43,** 65-85.
4 Lichtenthaler: *Zuckerindustrie,* 1991, **116,** 701 - 712.
5 Brown & Levy: *Acta Crystallogr., Sect. B.,* 1973, **29,** 790 - 797.
6 Hanson *et al.: Acta Crystallogr., Sect. B.,* 1973, **29,** 797 - 808.
7 Bock & Lemieux: *Carbohydr. Res.,* 1982, **100,** 63 - 74.
8 McCain & Markley: *Carbohydr. Res.,* 1986, **152,** 73 - 80.
9 McCain & Markley: *J. Am. Chem. Soc.,* 1986, **108,** 4259 - 4264.
10 Christofides & Davies: *J. Chem. Soc., Chem. Commun.,* 1985, 1533 - 1534.
11 Davies & Christofides: *Carbohydr. Res.,* 1987, **163,** 269 - 274.
12 Adams & Lerner: *J. Am. Chem. Soc.,* 1992, **114,** 4827 - 4829.
13 Stevens & Duda: *J. Am. Chem. Soc.,* 1991, **113,** 8622 - 8627.
14 du Penhoat *et al.: J. Am. Chem. Soc.,* 1991, **113,** 3720 - 3727.
15 Tran & Brady: *Biopolymers,* 1990, **29,** 961 - 976.
16 Tran & Brady: *Biopolymers,* 1990, **29,** 977 - 997.
17 Lichtenthaler *et al.: Starch/Starke,* 1992, **44,** 445 - 456.
18 French & Dowd: *J. Mol. Struct. (Theochem),* 1993, **286,** 183 - 201.
19 Lindner: PIMM - Closed Shell π –SCF-LCAO-MO-Molecular Mechanics Program. Technische Hochschule Darmstadt, **1988.** - Smith, & Lindner, J. *Comput. Aided Mol. Des.,* 1991, **5,** 235 - 262.
20 (a) Brickmann: MOLCAD - MOLecular Computer Aided Design.Technische Hochschule Darmstadt, **1992.** - The SYBYL-MOLCAD program package is an interactive, fast computer program for building and manipulating molecules and molecular systems. It is particularly suited to analyse and represent different physical molecular properties such as the electrostatic potential on three-dimensional solid molecular surfaces even of large molecules like proteins, zeolithes, and polymers. MOLCAD runs on Silicon-Graphics workstations and can be licensed from TRIPOS Associates, St. Louis, MO, USA.
(b) Brickmann: J. *Chim. Phys.,* 1992, **89,** 1709 - 1721.
(c) Waldherr-Teschner *et al.:"Advances in Scientific Visualization"* Eds. Post & Hin,(Springer Verlag, Heidelberg), 1992, pp. 58 - 67
21 Chauvin, *et al.: J. Org. Chem.,* 1993, **58,** 2291 - 2295.
22 Pokinskyj & Lichtenthaler: Unpublished results, 1994.
23 Hamann *et al.: J. Carbohydr. Chem.,* 1993, **12,** 173 - 190.
24 Lichtenthaler & Immel: *"Sweet-Taste Chemoreception"* Ed. Mathlouthi *et al.,* (Elsevier, New York) 1992, pp. 21 - 53.
25 Shallenberger & Acree: *Nature,* 1967, **216,** 480 - 482; *J. Agric. Food Chem.,* 1969, **17,** 701 - 703.
26 Kier: J. *Pharm. Sci.,* 1972, **61,** 1394 - 1397.
27 Lee: *Adv. Carbohydr. Chem. Biochem.,* 1987, **45,** 199 - 351.
28 Lancet & Ben-Arie, *"Sweeteners: Discovery, Molecular Design, and Chemoreception"* (Eds. Walter *et al.* Am. Soc., Washington, D.C., 1991, pp. 226 - 236.
29 Simon: *ibid.,* pp. 237 - 250.
30 Dubois*et al.*: *"Sweet-Taste Chemoreception"* (Eds. Mathlouthi *et al.,* (Elsevier, New York) 1992, pp. 237 - 267.
31 Faurion *"Sweet-Taste Chemoreception" ibid.,* pp. 291 - 315.
32 Mathlouthi & Portmann: *J. Mol. Struct.,* 1990, **237,** 327 - 338.
33 Mathlouthi & Seuvre: *J. Chem. Soc., Faraday Trans. 1,* 1988, **84,** 2641 - 2650.
34 Hough & Khan: *"Progress in Sweeteners"* (Ed. Grenby), (Elsevier, London), 1990, pp. 97 - 120.
35 Lichtenthaler & Immel: *"Sweet-Taste Chemoreception" Eds.* Mathlouthi *et al.* (Elsevier, New York), 1992, pp. 40 - 45.
36 Bart: *J. Chem. Soc., B,* 1968, 376 - 382.
37 Okaya: *Acta Crystallogr., Sect. B,* 1969, **25,** 2257 - 2263.
38 Paulus: *Acta Crystallogr., Sect. B,* 1975, **31,** 1191 - 1193.
39 Hatada *et al.: J. Am. Chem. Soc.,* 1985, **107,** 4279 - 4282.
40 Saenger: *Angew. Chem.,* 1980, **92,** 343 - 361; *Angew. Chem. Int. Ed. Engl.,* 1980, **19,** 344 - 362.
41 Wenz: *Angew. Chem.,* 1994, **106,** 851 - 870; *Angew. Chem. Int. Ed. Engl.,* 1994, 33, 803 - 822.
42 Chacko & Saenger: *J. Am. Chem. Soc.,* 1981, **103,** 1708 - 1715.
43 Zabel *et al.: J. Am. Chem. Soc.,* 1986, **108,** 3664 - 3673.
44 Harata: *Bull. Chem. Soc. Jpn.,* 1987, **60,** 2763 - 2767.
45 Fujiwara *et al.: Chem. Lett.,* 1990, 739 - 742.
46 Immel: *Dissertation,* Technische Hochschule Darmstadt, 1994.
47 Immel & Lichtenthaler: *Starch/Starke,* 1995, **47,** in press.
48 Kawamura *et al.: Carbohydr. Res.,* 1989, **192,** 83 - 90.
49 Uchiyama: *"Inulin and Inulin-containing Crops"* (Ed. Fuchs), (Elsevier, Amsterdam), 1993, pp. 143 - 148.
50 Sawada *et al.: Carbohydr. Res.,* 1991, **217,** 7 - 17.
51 Rappenecker & Zugenmaier: *Carbohydr. Res.,* 1981, **89,** 11 - 19.
52 Imberty,*et al.: J. Mol. Biol.,* 1988, **201,** 365 - 378.
53 Saito*et al.*: *Bull. Chem. Soc. Jpn.,* 1991, **64,** 3528 - 3537.
54 Carlson *et al.: Starch/Starke,* 1979, **31,** 222 - 224.
55 Bluhm & Zugenmaier: *Carbohydr. Res.,* 1981, **89,** 1 - 10.
56 Kanters *et al.: Carbohydr. Res.,* 1988, **180,** 175 - 182.